

## Short Communication

# In Vivo Binding of Protoporphyrin IX to Rat Translocator Protein Imaged With Positron Emission Tomography

HARUSHIGE OZAKI,<sup>1</sup> SAMI S. ZOGHBIL,<sup>1</sup> JINSOO HONG,<sup>1</sup> AJAY VERMA,<sup>2</sup> VICTOR W. PIKE,<sup>1</sup>  
ROBERT B. INNIS,<sup>1</sup> AND MASASHIRO FUJITA<sup>1\*</sup>

<sup>1</sup>Molecular Imaging Branch, National Institute of Mental Health, National Institutes of Health, Bethesda, Maryland

<sup>2</sup>VP Neuroscience and Ophthalmology, Novartis Pharmaceuticals Corporation, East Hanover, New Jersey

**KEY WORDS** peripheral benzodiazepine receptor; 5-aminolevulinic acid; porphyria

**ABSTRACT** In vitro experiments have shown that protoporphyrin IX (PPIX) binds to the translocator protein 18 kDa (TSPO), which transports cholesterol across the outer mitochondrial membrane. The purpose of this study was to examine whether binding of PPIX to TSPO can also be detected in vivo using positron emission tomography and [<sup>11</sup>C]PBR28, a radioligand that binds with high affinity and selectivity to TSPO. Rats were injected with a high dose of 5-aminolevulinic acid (ALA, 200 mg/kg i.v.), which is a precursor for PPIX. ALA-pretreatment significantly decreased the uptake of [<sup>11</sup>C]PBR28 in TSPO-rich organs such as heart, kidneys, lungs, parotid glands, and spleen by 57–80%. As a control experiment, injection of a receptor saturating dose of PK 11195, which is selective for TSPO, produced a pattern of displacement similar to that after ALA but with greater magnitude (88–97%). This study provides the first evidence that PPIX binds in vivo to TSPO. Although PPIX at physiological concentrations would likely occupy an insignificant percentage of TSPOs, it does reach high-enough concentrations in porphyria to occupy and have pharmacological effects via this target. **Synapse 64:649–653, 2010.** © 2010 Wiley-Liss, Inc.

Among several proposed functions, translocator protein 18 kDa (TSPO) transports cholesterol across the outer mitochondrial membrane to an enzyme (CYP11A1), which converts cholesterol into pregnenolone, a common precursor for steroids (Papadopoulos et al., 2006). TSPO was first detected in kidney and was originally called the peripheral benzodiazepine receptor. TSPO may be a useful biomarker for inflammation, because it is highly expressed in phagocytic inflammatory cells, such as activated microglia in brain and macrophages in the periphery (Banati, 2003).

Positron emission tomographic (PET) radioligands selective for TSPO can localize inflammation (activated microglia) in several brain disorders, including multiple sclerosis, stroke, and Alzheimer's disease (Venneti et al., 2006). Our laboratory recently discovered that about 10% of the population show no specific binding to TSPO using [<sup>11</sup>C]PBR28, a PET radioligand with high affinity and selectivity for TSPO (Fujita et al., 2008. Results of the absence of specific binding in a larger sample size have not been published.). Results of absence of specific binding in a larger sample size have not been published. One potential cause of this nonbinding is an excessive

amount of an endogenous compound that binds to TSPO and displaces the radioligand.

The major endogenous porphyrin, protoporphyrin IX (PPIX), binds to TSPO and can displace [<sup>3</sup>H]PK 11195, with in vitro IC<sub>50</sub> values reported from 0.015 to 19  $\mu$ M (Ferrarese et al., 1990; Verma et al., 1987, 1998; Wendler et al., 2003). Since PK 11195 and PBR28 both fully displace each other, in vivo concentrations of PPIX might be high enough to displace [<sup>11</sup>C]PBR28 in nonbinders. Based on in vitro studies, PPIX is a substrate for TSPO, which may play a role in heme biosynthesis (Wendler et al., 2003). In addition, porphyrins have been used as photosensitive agents in experimental cancer therapies. TSPOs are

Contract grant sponsor: Intramural Program, NIMH; Contract grant numbers: Z01-MH-002795-07, Z01-MH-002793-07.

\*Correspondence to: Masahiro Fujita, Molecular Imaging Branch, National Institute of Mental Health, Building 31, Room B2B37, 31 Center Drive, MSC-2035, Bethesda, MD 20892-2035, USA. E-mail: fujitam@intram.nih.gov

Received 21 September 2009; Accepted 30 December 2009

DOI 10.1002/syn.20779

Published online 23 March 2010 in Wiley InterScience (www.interscience.wiley.com).

highly expressed in some cancer cells and UV light causes porphyrins to bind to TSPOs and thereby induce toxicity (Verma et al., 1998).

Since porphyrins are known to bind to TSPOs in vitro, we examined whether an adequate concentration of porphyrins can be achieved in vivo to block almost all radioligand specific binding to TSPO, and so provide a possible explanation for the "nonbinder phenomenon." It is not common to administer PPIX for in vivo studies, and a common method to increase PPIX levels in vivo is to administer a precursor, 5-aminolevulinic acid (ALA). In addition, tissue concentrations of PPIX after ALA administration have been reported (van den Boogert et al., 1998). Therefore, we administered ALA to increase tissue concentrations of PPIX to the range of its  $K_i$  values. The dose of ALA used in this study increases in vivo concentrations of PPIX by 2.5- to 15-fold in TSPO-rich organs (van den Boogert et al., 1998). We imaged rats with [ $^{11}\text{C}$ ]PBR28 and compared the effects of ALA with that of a high dose of PK 11195, which is known to block virtually all TSPOs in the body.

## MATERIALS AND METHODS

### Chemicals

*N*-Acetyl-*N*-(2-[ $^{11}\text{C}$ ]methoxybenzyl)-2-phenoxy-5-pyridinamine ([ $^{11}\text{C}$ ]PBR28) was synthesized as previously described (Briard et al., 2008). The specific activity of [ $^{11}\text{C}$ ]PBR28 at time of injection was  $119 \pm 45$  GBq/ $\mu\text{mol}$  (mean  $\pm$  SD). PK 11195 (racemic) and 5-ALA were purchased from Sigma-Aldrich (St. Louis, MO).

### Animals

Male Sprague-Dawley rats (320 g, Taconic, Hudson, NY) were divided into three groups: control, ALA- and PK 11195-pretreatment. ALA (200 mg/kg i.v.) or saline was i.v. injected 2 h before PET scanning. This dose of ALA produces plasma and organ PPIX peak levels of 0.5–20  $\mu\text{M}$  (van den Boogert et al., 1998), which is comparable with the  $\text{IC}_{50}$  values (Ferrarese et al., 1990; Verma et al., 1987, 1998; Wendler et al., 2003). For comparison, a receptor-saturating dose of PK 11195 (10 mg/kg i.v.) was injected 2 min before PET scanning. Animals were anesthetized by 2% isoflurane and 98% oxygen 1–1.5 h before and during the PET scan. Under anesthesia, polyethylene tubes (PE-10) were inserted in the femoral artery to sample blood and in the tail vein to inject [ $^{11}\text{C}$ ]PBR28. Body temperature was monitored with a rectal probe maintained at about 38°C with warm air. All procedures were performed in compliance with Guide for Care and Use of Laboratory Animals and were approved by NIMH Animal Care and Use Committee.

### PET scan

We used the High Resolution Research Tomograph (HRRT, Siemens/CPS, Knoxville, TN), which has a reconstructed resolution of 2.5 mm full-width half-maximum. Two animals were scanned simultaneously for 2 h, beginning with a 6-min infusion of [ $^{11}\text{C}$ ]PBR28 ( $45 \pm 10$  MBq for control;  $45 \pm 11$  MBq for ALA-pretreated;  $48 \pm 4$  MBq for PK 11195-pretreated).

### Measurement of radioligand concentration in plasma

Arterial blood was sampled eight times between 0 and 10 min and at 20, 40, 60, and 120 min and was put in heparin-coated tubes. In all animals, total activity in plasma was measured with a calibrated gamma counter. In addition, in one of two animals for each scan, [ $^{11}\text{C}$ ]PBR28 concentrations in plasma were measured with radio-reversed phase high-performance liquid chromatography (HPLC) (radio-HPLC). Because we administered PPIX in the same way as reported previously where organ PPIX levels were reported (van den Boogert et al., 1998), we did not measure plasma PPIX levels in this study to limit volume of blood sampling.

### Image analysis

Image data were reconstructed in 33 frames with durations ranging from 30 s to 5 min. Regions of interest were individually defined on the PET image for the entire brain, heart, kidneys, liver, lungs, parotid glands, neck skeletal muscles, and spleen. To normalize organ uptake relative to injected activity and body weight, concentration of activity in organs was expressed as standardized uptake value (SUV), calculated as the fraction of injected activity per cubic centimeters organ  $\times$  body weight (in grams). The area under the curve (AUC) for all the organs except for the brain were calculated by the trapezoidal method and then normalized to AUC of plasma total activity (organ AUC/plasma AUC). Image analysis was performed using PMOD 2.95 (pixelwise modeling software; PMOD Technologies, Zurich, Switzerland).

### Measurement of distribution volume in brain

Total distribution volume ( $V_T$ ), which reflects  $B_{\text{max}}/K_D$ , was measured using metabolite-corrected arterial input function and by applying nonlinear least-squares fitting with an unconstrained two compartment model in PMOD 2.95. The identifiability of the kinetic variables was calculated as the standard error (SE) from the diagonal of the covariance matrix of nonlinear least-squares fitting.

### Statistics

Data are expressed as mean  $\pm$  SD. Statistical analyses were performed on two outcome measures: organ AUC/plasma AUC and  $V_T$  in the control and ALA-pretreated groups. Parametric and nonparametric variables were determined by the Shapiro–Wilk normality or Kolmogorov–Smirnov test. The statistical significance of differences was determined using unpaired Student's *t*-test (parametric) or the Mann–Whitney (nonparametric) test. *P*-values of less than 0.05 were considered to be statistically significant.

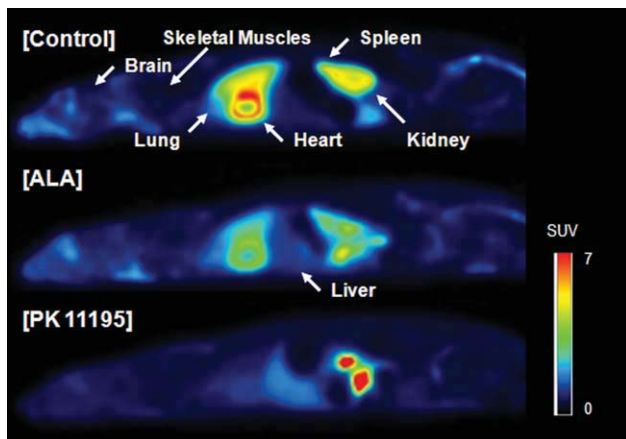


Fig. 1. [ $^{11}\text{C}$ ]PBR28 PET images of control, ALA-pretreated, and PK 11195-pretreated rats. The images were averaged from 0 to 120 min after injection, and the concentration of activity was expressed as SUV. On these sagittal images, the head is on the left. ALA and PK 11195 decreased uptake of [ $^{11}\text{C}$ ]PBR28 in TSPO-rich organs. In the PK 11195-pretreated rat, high activity was seen in the intestine and the pelvis of the kidney presumably due to faster excretion.

### RESULTS

Control scans with [ $^{11}\text{C}$ ]PBR28 showed high uptake of activity in organs known to have high densities of TSPO (Anholt et al., 1985; Fookes et al., 2008; Matarrese et al., 2001): heart, kidneys, lungs, and spleen (Fig. 1). Despite an increase in plasma total activity, ALA-pretreatment substantially decreased uptake in these four target organs (Figs. 1 and 2). The ALA-induced increase of plasma total activity was consistent with its causing blockade of TSPOs. We have shown that blockade of binding to TSPOs in peripheral tissue blunts the distribution of radioligand to these tissues, thereby elevating plasma concentration of the radioligand (Imaizumi et al., 2008).

To calculate the percentage blockade induced by ALA and to compensate for the greater exposure to the organs from the increased concentration of radioligand in plasma, we normalized organ activity to plasma total activity as organ AUC/plasma AUC. ALA-pretreatment markedly decreased uptake in heart by 80%, kidneys, lungs by 76%, parotid glands by 70%, and spleen by 57% ( $P < 0.0001$  for all of these organs (Fig. 3). Small decreases were also noted in the liver and skeletal muscles (26 and 38%, respectively) (Fig. 3), which have low density of TSPO (Anholt et al., 1985; Fookes et al., 2008; Matarrese et al., 2001). Magnitude of the decrease largely correlated with the density of TSPO, indicating that specific binding of [ $^{11}\text{C}$ ]PBR28 was blocked. From these results, the suppression effects noted in this study indicate competitive binding of PPIX with the PET ligand at TSPO. As a positive control experiment, the selective ligand PK 11195 (10 mg/kg i.v.) blocked

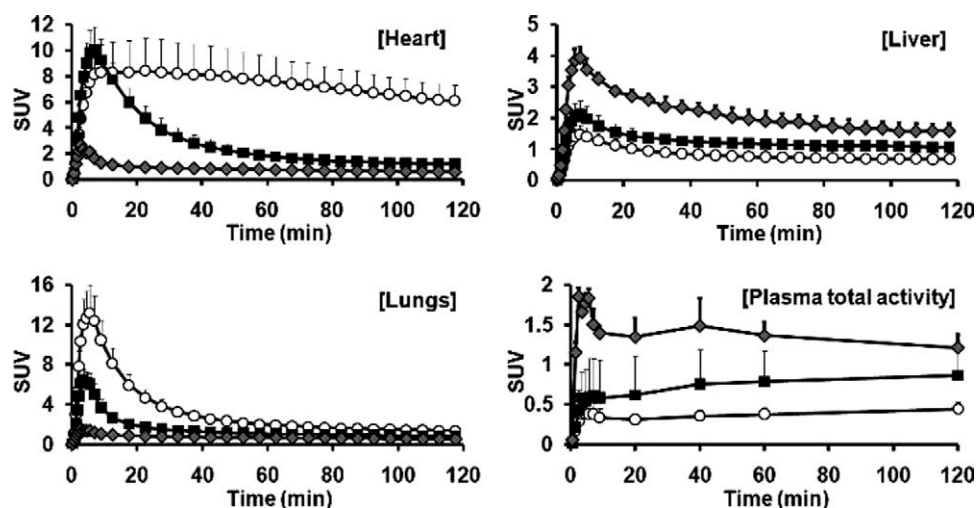


Fig. 2. Time-activity curves of TSPO-rich (heart and lung), TSPO-poor organs (liver), and plasma total activity after [ $^{11}\text{C}$ ] PBR28 injection in control ( $\circ$ ), ALA-pretreated ( $\blacksquare$ ), and PK 11195-pretreated ( $\blacklozenge$ ) groups. Each value is expressed as the mean plus SD of 14, 12, and 3 animals for the control, ALA, and PK 11195 groups, respectively. Plasma total activity in plasma was the mean of 12, 11, and 3 animals, respectively.



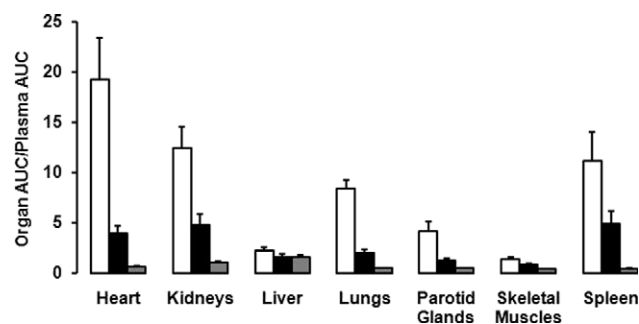


Fig. 3. Uptake of activity in organs of the rat after injection of [ $^{11}\text{C}$ ]PBR28. The uptake was calculated as the area under the curve (AUC) for the 2 h of imaging after injection and was normalized to the AUC of plasma total activity during the same period. The bar and associated error bar are mean and SD from control ( $\square$ ,  $n = 12$ ), ALA-pretreated ( $\blacksquare$ ,  $n = 11$ ), and PK 11195-pretreated ( $\blacksquare$ ,  $n = 3$ ) rats. The differences between control and ALA-pretreated groups were statistically significant for every organ (liver,  $P = 0.0035$ ; others,  $P < 0.0001$ ). Data for PK 11195 were not analyzed statistically, because only three animals were injected in this group.

uptake in these same organs but by a higher percentage (88–97%) than for ALA (57–80%) (Fig. 3).

Because of the interest to use [ $^{11}\text{C}$ ]PBR28 to localize neuroinflammation, we performed full quantification of brain activity by compartmental modeling and using the metabolite-corrected arterial input function. PK 11195-pretreatment decreased brain total distribution volume ( $V_T$ ) by 77%, confirming that [ $^{11}\text{C}$ ]PBR28 had specific binding in rat brain (Table I). However, ALA decreased  $V_T$  in brain by only 14%, which was statistically insignificant ( $P = 0.61$ , Table I).

## DISCUSSION

By increasing PPIX levels with the administration of the precursor ALA, we showed that PPIX binds in vivo to TSPO and displaces the selective PET radioligand [ $^{11}\text{C}$ ]PBR28. As expected for binding to TSPO, the effect of ALA was greatest for those organs with the highest densities of TSPO. The pattern of organs affected by ALA was similar to that after blockade by the selective TSPO ligand PK 11195. However, the effect of ALA (200 mg/kg) was about 70% of that of PK 11195 administered at receptor-saturating dose (10 mg/kg i.v.). A possible reason for the difference between ALA and PK 11195 was that PPIX levels produced by the dose of ALA were not high enough to saturate binding to TSPO.

Although our results show that high doses of ALA, presumably via its conversion into porphyrins, can bind in vivo to substantial percentage of TSPOs, these endogenous ligands are unlikely to have significant effects on PET imaging in healthy subjects. ALA induced about 60–80% receptor occupancy in the four large organs with high densities of TSPO (heart, kidneys, lungs, and spleen). This dose of ALA (200 mg/kg i.v.) induces about 7-fold (ranging 2.5- to 15-fold)

TABLE I. Distribution volume ( $V_T$ ) of [ $^{11}\text{C}$ ]PBR28 for the brain in the control, ALA-pretreated, and PK 11195-pretreated groups

Group	$n$	$V_T$ (mL/cm $^3$ )	Decrease (%)
Control	6	$66 \pm 24$	—
ALA	5	$57 \pm 30$	14
PK 11195	2	15	77

Total distribution volume ( $V_T$ ) was measured using an unconstrained two-tissue compartment model and metabolite-corrected arterial input function. The values of  $V_T$  were insignificantly different ( $P = 0.61$ ) between control and ALA-pretreated groups. The PK 11195 data were not analyzed statistically because only two animals were in this group.

increase of tissue PPIX in TSPO-rich organs. Assuming a simple linear relationship (which does not account for the known saturability of this receptor), the occupancy of TSPO by PPIX at baseline in rats and in healthy humans would be 10% (70/7). Furthermore, the virtually complete blockade of TSPO binding we found in about 10% of healthy subjects could not have been caused by elevated porphyrins. However, the plasma concentrations of PPIX in patients with erythropoietic porphyria (0.18–8  $\mu\text{M}$ ) (Eichbaum et al., 2005; Poh-Fitzpatrick et al., 2002) are within the range of in vitro  $\text{IC}_{50}$  values PPIX to displace [ $^3\text{H}$ ]PK 11195 (0.015–19  $\mu\text{M}$ ) and are comparable with the plasma concentration of PPIX in rats after this dose of ALA (1.5  $\mu\text{M}$ ) (van den Boogert et al., 1998). Thus, patients with porphyria may have high enough tissue concentrations of PPIX to block binding of [ $^{11}\text{C}$ ]PBR28, and PPIX might even induce some pathophysiological effects via TSPO.

Although ALA pretreatment significantly blocked TSPOs in peripheral organs by 57–80%, it insignificantly blocked TSPOs in brain by only 14%. Two reasons for the small effect in brain are: (1) PPIX levels after ALA administration in brain are  $\sim 10$ -fold lower than those in rat TSPO-rich organs (van den Boogert et al., 1998). (2) Our calculation of distribution volume  $V_T$  in brain had significant noise. The values of SE were higher (mean  $\sim 18\%$ ) than that preferred in compartmental modeling ( $<10\%$ ) and indicated poor identifiability of the parameter. Thus, a larger sample size may show a significant effect.

In conclusion, this study provides the first evidence that PPIX can bind in vivo to TSPO, as evidenced by blockade of the TSPO-selective radioligand [ $^{11}\text{C}$ ]PBR28. Although PPIX may reach high enough concentrations in patients with porphyria to occupy a significant percentage of TSPOs, its concentration in healthy subjects is likely to have a negligible effect and could not explain the phenomenon of almost complete nonbinding to [ $^{11}\text{C}$ ]PBR28 found in about 10% of healthy subjects.

## ACKNOWLEDGMENTS

The authors thank Kimberly Jenko and Kacey Anderson for their assistance in measuring metabolite-corrected arterial input function, Jieih-San Liow

for image processing, and PMOD Technologies (Zurich, Switzerland) for providing its image analysis and modeling software.

## REFERENCES

- Anholt RRH, De Souza EB, Oster-Granite ML, Snyder SH. 1985. Peripheral-type benzodiazepine receptors: Autoradiographic localization in whole-body sections of neonatal rats. *J Pharmacol Exp Ther* 233:517–526.
- Banati RB. 2003. Neuropathological imaging: In vivo detection of glial activation as a measure of disease and adaptive change in the brain. *Br Med Bull* 65:121–131.
- Briard E, Zoghbi SS, Imaizumi M, Gourley JP, Shetty HU, Hong J, Cropley V, Fujita M, Innis RB, Pike VW. 2008. Synthesis and evaluation of two sensitive  $^{11}\text{C}$ -labeled aryloxyanilide ligands for imaging brain peripheral benzodiazepine receptors in vivo. *J Med Chem* 51:17–30.
- Eichbaum QG, Dzík WH, Chung RT, Szczepiorkowski ZM. 2005. Red blood cell exchange transfusion in two patients with advanced erythropoietic protoporphyria. *Transfusion* 45:208–213.
- Ferrarese C, Appollonio I, Frigo M, Perego M, Pierpaoli C, Trabucchi M, Frattola L. 1990. Characterization of peripheral benzodiazepine receptors in human blood mononuclear cells. *Neuropharmacology* 29:375–378.
- Fookes CJR, Pham TQ, Mattner F, Greguric I, Loc'h C, Liu X, Berghofer P, Shepherd R, Gregoire MC, Katsifis A. 2008. Synthesis and biological evaluation of substituted  $^{18}\text{F}$ -imidazo[1,2-*a*]pyridines and  $^{18}\text{F}$ -pyrazolo[1,5-*a*]pyrimidines for the study of the peripheral benzodiazepine receptor using positron emission tomography. *J Med Chem* 51:3700–3712.
- Fujita M, Imaizumi M, Zoghbi SS, Fujimura Y, Farris AG, Suhara T, Hong J, Pike VW, Innis RB. 2008. Kinetic analysis in healthy humans of a novel positron emission tomography radioligand to image the peripheral benzodiazepine receptor, a potential biomarker for inflammation. *NeuroImage* 40:43–52.
- Imaizumi M, Briard E, Zoghbi SS, Gourley JP, Hong J, Fujimura Y, Pike VW, Innis RB, Fujita M. 2008. Brain and whole-body imaging in nonhuman primates of  $^{11}\text{C}$ -PBR28, a promising PET radioligand for peripheral benzodiazepine receptors. *NeuroImage* 39:1289–1298.
- Matarrese M, Moresco RM, Cappelli A, Anzini M, Vomero S, Simonelli P, Verza E, Magni F, Sudati F, Soloviev D, Todde S, Carpinelli A, Kienle MG, Fazio F. 2001. Labeling and evaluation of *N*- $^{11}\text{C}$ -methylated quinoline-2-carboxamides as potential radioligands for visualization of peripheral benzodiazepine receptors. *J Med Chem* 44:579–585.
- Papadopoulos V, Baraldi M, Guilarte TR, Knudsen TB, Lacapère JJ, Lindemann P, Norenberg MD, Nutt D, Weizman A, Zhang MR, Gavish M. 2006. Translocator protein (18 kDa): New nomenclature for the peripheral-type benzodiazepine receptor based on its structure and molecular function. *Trends Pharmacol Sci* 27:402–409.
- Poh-Fitzpatrick MB, Wang X, Anderson KE, Bloomer JR, Bolwell B, Lichtin AE. 2002. Erythropoietic protoporphyria: Altered phenotype after bone marrow transplantation for myelogenous leukemia in a patient heteroallelic for ferrochelatase gene mutations. *J Am Acad Dermatol* 46:861–866.
- van den Boogert J, van Hillegersberg R, de Rooij FWM, de Bruin RWF, Edixhoven-Bosdijk A, Houtsmuller AB, Siersema PD, Wilson JH, Tilanus HW. 1998. 5-Aminolaevulinic acid-induced protoporphyria IX accumulation in tissues: Pharmacokinetics after oral or intravenous administration. *J Photochem Photobiol B* 44:29–38.
- Venneti S, Lopresti BJ, Wiley CA. 2006. The peripheral benzodiazepine receptor (Translocator protein 18 kDa) in microglia: From pathology to imaging. *Prog Neurobiol* 80:308–322.
- Verma A, Facchina SL, Hirsch DJ, Song S-Y, Dillahey LF, Williams JR, Snyder SH. 1998. Photodynamic tumor therapy: Mitochondrial benzodiazepine receptors as a therapeutic target. *Mol Med* 4:40–45.
- Verma A, Nye JS, Snyder SH. 1987. Porphyrins are endogenous ligands for the mitochondrial (peripheral-type) benzodiazepine receptor. *Proc Natl Acad Sci USA* 84:2256–2260.
- Wendler G, Lindemann P, Lacapère J-J, Papadopoulos V. 2003. Protoporphyrin IX binding and transport by recombinant mouse PBR. *Biochem Biophys Res Commun* 311:847–852.